PAPER

Detection of Epstein–Barr virus infection in cancer by using highly specific nanoprobe based on dBSA capped CdTe quantum dots†

Yilin Li,[ab] Lihong Jing,[b] Ke Ding,[b] Jing Gao,[a] Zhi Peng,[a] Yanyan Li,[a] Lin Shen*[a] and Mingyuan Gao*[b]

By using denatured bovine serum albumin (dBSA) molecules as multidentate ligands, surface-functionalized CdTe quantum dots (QDs) were synthesized and further evaluated for preparing fluorescent probes capable of detecting Epstein–Barr virus infection. The optical studies revealed that the dBSA coating effectively improved the optical stability of the resulting QDs (CdTe@dBSA). The interaction between CdTe@dBSA and the membrane of carcinoma cells further suggested that the nonspecific adsorption of CdTe QDs stabilized by thioglycolic acid (TGA) was significantly eliminated upon the dBSA coating. Streptavidin was covalently conjugated to CdTe@dBSA to endow the QDs with specific binding affinity in detecting the serum level of anti-Epstein–Barr virus (EBV) capsid antigen IgA (VCA-IgA) in nasopharyngeal carcinoma patients for early screening and diagnosing EBV-associated cancers.

1. Introduction

Quantum dots (QDs) have been attracting considerable attention owing to their unique electronic and optical properties.[1–3] As the spectral features of QDs – in comparison with that of conventional dyes – is characterized by narrow, symmetric, and particle size-dependent fluorescence, as well as a broad excitation range and excellent robustness against photobleaching, QDs are ideal on many counts for bioassay and bioimaging.[2–7] However, due to the strong surface defect-sensitive fluorescence, the emission intensity of QDs only coated with a small thiol ligand, such as thioglycolic acid (TGA), mercaptopropionic acid (MPA), and so forth, is readily reduced in physiological environments.[8–10] Most importantly, the surface of the QDs is always prone to adsorbing biomolecules nonspecifically,[11–13] which sharply decreases the specificity of the QDs-based molecular probes, and thereby limits the bioapplication of QDs.

Several strategies for surface modification on QDs have been developed to overcome these drawbacks.[14–20] However, the major

[a]Key Laboratory of Carcinogenesis and Translational Research (Ministry of Education), Department of GI Oncology, Peking University Cancer Hospital and Institute, Fucheng Road 52, Haidian District, Beijing 100142, China. E-mail: lin100@medmail.com.cn; Tel: +86-10-88196561

[b]Institute of Chemistry, the Chinese Academy of Sciences, Bei Yi Jie 2, Zhong Guan Cun, 100190 Beijing, China. E-mail: gaomy@iccas.ac.cn; Tel: +86-10-82613214

† Electronic supplementary information (ESI) available: The fluorescence intensity and peak position of CdTe@dBSA with different dBSA : QD ratios, and the optical stability of CdTe@dBSA by optimal dBSA : QD ratio in 1× PBS are respectively shown in Fig. S1 and S2; the fluorescent stability of CdTe@dBSA–streptavidin bioconjugate are shown in Fig. S3. See DOI: 10.1039/c4ra02277g

strategies, such as the encapsulation of QDs with silica,[21–23] organic polymers,[24–27] or amphiphilic polymers[15,17,18,20] have concentrated on passivating the surface defects of QDs thereby improving their fluorescence stability.[26,28] Limited approaches have been developed to suppress the nonspecific interaction between QDs and biomolecules. Polyethylene glycol (PEG) remains the most commonly used material to modify the surface of nanoparticles for suppressing their non-specific adsorption with biomolecules.[5,14,29] Owing to the antifouling property of PEG, the binding specificity of PEG-coated particle probes can be effectively improved for immunofluorescence assays.[5,30] Even for *in vivo* applications, PEG-coated QDs also exhibit reduced nonspecific accumulation in the reticuloendothelial tissues, which is beneficial for increasing the accumulation of QDs at region of interest.[12] In addition, multidentate PEG ligands have also been developed for effectively passivating the surface defects.[15–19,31] However, the preparation of multidentate PEG ligands requires sophisticated synthetic procedures. Moreover, the functional groups, typical at the end of the PEG molecules, limit the number of bioligands to conjugate to PEGylated QDs, and thereby their potential in bioassays and bioimaging.[30]

Denatured bovine serum albumin (dBSA) has recently been used to manipulate the surface chemistry of QDs.[32,33] Prepared by chemically reducing disulfide bonds in BSA, dBSA contains 37 thiol groups per monomer, thereby affording them great potential as excellent multidentate ligands for nanoparticles. Apart from that, BSA is also a well-known blocking reagent to reduce nonspecific adsorption in immunoassays similar to PEG.[34–36] It is therefore reasonable to expect that dBSA as multidentate ligands can not only passivate surface defects and improve the optical properties of QDs, but also suppress the

nonspecific interaction of QDs with biomolecules. Moreover, compared with PEG polymer, dBSA contains different functional groups such as amino and carboxyl groups along the polymer backbone, which provides more reactive sites for conjugation with bioligands to achieve QD-based probes for both bioassay and bioimaging.

Following this rationale, dBSA was chosen to encapsulate CdTe QDs stabilized by TGA in this study. The optical properties of the resulting CdTe@dBSA were systematically studied. The interaction between CdTe@dBSA and carcinoma cells was then studied to investigate the resistance of dBSA coating to non-specific binding. Furthermore, the CdTe@dBSA–streptavidin conjugate was synthesized and used as a molecular probe to detect Epstein–Barr virus (EBV) infection in nasopharyngeal carcinoma (NPC) patients. EBV, as a member of the herpes virus family, has been implicated in the occurrence of various cancers, such as NPC, Burkitt's lymphoma, gastric carcinoma, and so forth.[37] After infected by EBV, patients always exhibit elevated level of anti-EBV antibodies in sera, particularly the anti-EBV capsid antigen IgA (VCA-IgA).[37–39] Therefore, detection of the serum level of VCA-IgA has served as an effective strategy for early screening and diagnosis of EBV-associated cancers.[38,39] In this paper, the application of the CdTe@dBSA–streptavidin conjugate in detecting the serum level of VCA-IgA in NPC patients was also demonstrated through indirect immunofluorescence assays.

2. Materials and methods

2.1. Chemicals

Aluminum telluride (Al_2Te_3, 99.5%), cadmium perchlorate hydrate ($Cd(ClO_4)_2 \cdot 6H_2O$, 99.9%), thioglycolic acid (TGA, 97+%), 1-ethyl-3-(3-dimethylaminopropyl) carbodiimide (EDC, 97.0+%), N-hydroxysulfo-succinimide sodium salt (Sulfo-NHS, 98.5%), were all purchased from Sigma-Aldrich. Agarose (Biowest Agarose) was purchased from Gene Tech. Co., Ltd., Shanghai, China. Streptavidin was purchased from Promega Biotech Co., Ltd. Bovine serum albumin (BSA, Amresco, 99%), acrylamide (AM, Amresco, 99+%), N,N'-methylenebis(acrylamide) (MBA, Amresco, 99%), ammonium persulfate (APS, Amresco, 95%), N,N,N',N'-tetramethylethylenediamine (TEMED, Sigma, 99%), tris(hydroxymethyl)aminomethane (Tris, Amresco, 99.9%), glycine (Gly, Amresco, 98.0%) were distributed by Biodee Biotechnology Co., Ltd., Beijing, China. Goat anti-human immunoglobulin A antibody (antiIgA Ab) was gifted from the National Institute for Viral Disease Control and Prevention, China CDC. Other chemicals were all purchased by Beijing Chemical Factory, Beijing, China. All the chemicals mentioned above were used as received.

2.2. Synthesis of CdTe QDs

Aqueous CdTe QDs stabilized by TGA were synthesized, by the reaction between Cd^{2+} and H_2Te, according to the method reported previously.[23,40–42] However, in the present study the initial pH of the precursor solution was set to 12 and the ratio of Cd : HSR was adjusted from 1 : 2.4 to 1 : 1.3. The resulting CdTe QDs with emission wavelength centered at 610 nm was used in the following investigations.

2.3. Preparation of CdTe@dBSA QDs

dBSA was prepared according to previous reports.[32,33,43] Briefly, $NaBH_4$ was added to BSA solution and reacted under stirring for 1 h. Then, the resultant solution was further heated to 60–80 °C until no more gas (H_2) was generated, in order to decompose the excess $NaBH_4$. Under these conditions, most of the disulfide bonds of BSA were reduced to thiol groups. The resultant dBSA solution was dialyzed against PBS buffer, and stored at 4 °C for further use.

For preparing CdTe@dBSA QDs, the dBSA was mixed with TGA-coated CdTe QDs in 1 × PBS to exchange the TGA ligands. This ligand exchange reaction typically lasted for 24 h at room temperature. The preparation of dBSA and CdTe@dBSA was carried out under anaerobic condition. After that, excess dBSA was removed by centrifugal ultrafiltration using Amicon 100 KD centrifugal ultrafiltration units (Millipore). The finally prepared CdTe@dBSA was characterized using 10% sodium dodecyl sulfate-polyacrylamide gel electrophoresis (SDS-PAGE).

2.4. Preparation of CdTe@dBSA–streptavidin bioconjugate

Before the conjugation reaction, the dBSA coating on CdTe QDs was succinylated by using succinic anhydride to convert the primary amine groups to carboxyl groups according to the protocol reported by Kuo *et al.*[33] The resulting succinylated CdTe@dBSA was activated in 1× PBS buffer containing EDC and sulfo-NHS (CdTe@dBSA : EDC : sulfo-NHS = 1 : 1000 : 2500) for 15 min under gentle stirring. Then streptavidin was introduced (CdTe@dBSA : streptavidin = 1 : 2 or 1 : 1) under gentle mixing for 4 h in 1× PBS. The resulting CdTe@dBSA–streptavidin bioconjugate was centrifuged by using Amicon 100 KD centrifugal ultrafiltration units to remove unreacted streptavidin, and then stored at 4 °C for 24 h before further characterization.

2.5. Detection of VCA-IgA in NPC patients

The indirect immunofluorescence method was adopted to detect VCA-IgA in the sera of NPC patients and healthy donors. In detail, the EBV-activated human lymphoma Raji cells (gifts from National Institute for Viral Disease Control and Prevention, China CDC) were fixed on glass slides. The sera diluted by a factor of 5 were introduced for incubating with the cells at 37 °C for 30 min. After that, the biotinylated antiIgA Ab was added after the cells were washed 3 times by using 1× PBS. The following incubation at 37 °C was allowed for another 30 min. After being washed 3 times with 1× PBS, the cell slide was subjected to incubation with the CdTe@dBSA–streptavidin bioconjugate at room temperature for 30 min. The cells finally obtained were imaged under Olympus IX71 inverted fluorescence microscope after being washed with 1× PBS.

3. Results and discussion

3.1. dBSA-coated CdTe QDs

The absorption and fluorescence spectra of the as-prepared CdTe QDs stabilized by TGA, denoted as CdTe@TGA, are shown in Fig. 1a. The room temperature fluorescence quantum yield (QY) was estimated to be ∼61% according to literature methods.[44,45] Representative transmission electron microscope (TEM) and high-resolution TEM (HRTEM) images of the CdTe@TGA QDs are shown in Fig. 1b. The average size of the QDs is around 3.5 nm according to the particle size histogram shown in Fig. 1c.

To confirm the formation of the CdTe@dBSA QDs by the ligand exchange reaction, 10% SDS-PAGE was carried out and the results are shown in Fig. 2a and b. The luminescent results reveal that the CdTe@dBSA (Lane 2) migrates far more slowly than CdTe@TGA QDs (Lane 1), implying the effective coating of dBSA on CdTe QDs. Further silver staining results as presented in Fig. 2b show that both dBSA (Lane 3) and CdTe@dBSA are stained owing to the existence of dBSA. According to previous studies,[32] the three bands of dBSA showing according to the silver staining results can be attributed to dBSA monomer, dBSA–dBSA dimer, and globulins, respectively. Since the first two bands of CdTe@dBSA exhibited by both fluorescence and silver staining match perfectly, it can be concluded that CdTe

Fig. 2 The fluorescence (a) and bright field silver staining (b) images of gel electrophoresis of CdTe@TGA (Lane 1), CdTe@dBSA (Lane 2), and dBSA (Lane 3). (c) The fluorescence spectra of CdTe@TGA (A), CdTe@dBSA (B), and the mixture of CdTe@TGA and BSA (C).
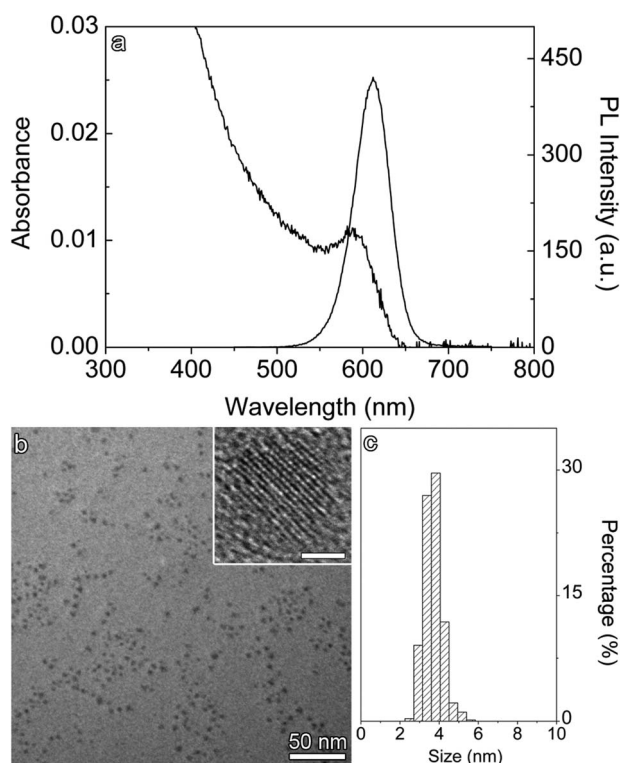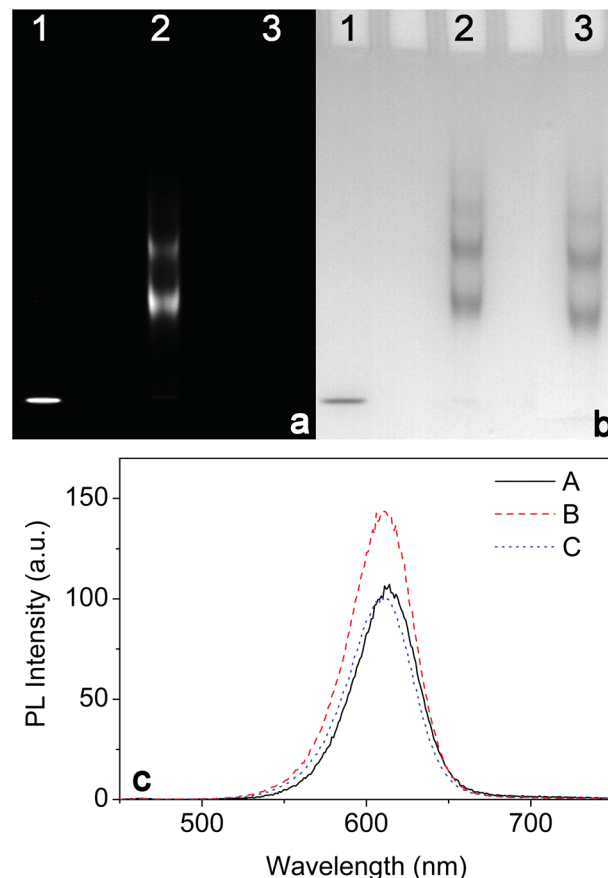

Fig. 1 Absorption and fluorescence spectra of the as-prepared CdTe QDs used in current investigations (a), the excitation wavelength for the fluorescence measurement was 360 nm; TEM and HRTEM (inset) image of CdTe QDs, the embedded scale bar in the inset corresponds to 2 nm (b); size histogram of the CdTe QDs according TEM measurements (c).

QDs coated by the monomer and dimer of dBSA were successfully obtained.

Further fluorescence studies suggest that the dBSA coating significantly increases the fluorescence intensity of the underlying CdTe core, as shown in Fig. 2c. In contrast, such enhancement effect was not presented upon simple mixing of BSA with CdTe@TGA QDs. On the contrary, the fluorescence intensity of the CdTe@TGA QDs is slightly decreased. These results support that dBSA can effectively passivate the CdTe core by eliminating of the surface defects.[32] In addition, dBSA molecule contains a large number of thiol groups, which is very helpful for eliminating the Cd-related defects.

To achieve high performance CdTe@dBSA for immunofluorescence assay, the effect of the dBSA-to-QDs ratio on fluorescence was studied. The results shown in Fig. 3a reveal that fluorescence intensity of the CdTe@dBSA increases with dBSA : QD ratio and then reaches a plateau when the dBSA-to-QD ratio is above 6 : 1. Thereby, the fluorescence intensity is enhanced by 35%. Further increasing the ratio above 20 : 1, the fluorescence intensity is slightly decreased. The results shown in Fig. 3a and ESI Fig. S1† however suggest that the fluorescence peak position is insensitive to the dBSA : QD ratio, suggesting that the size of the CdTe core is not altered by the surface dBSA modification.
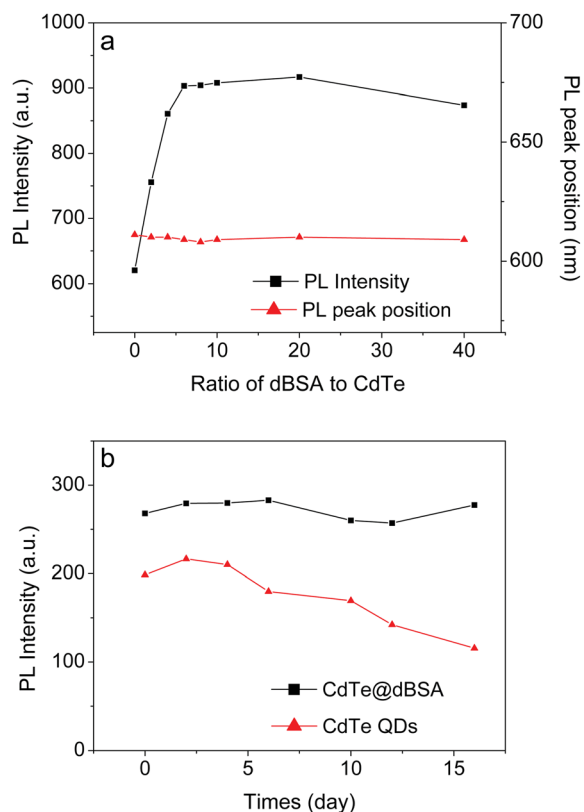
Fig. 3 (a) Fluorescence intensity and fluorescence peak position of CdTe@dBSA samples obtained by different dBSA : QD ratios. (b) Temporal fluorescence intensity of CdTe@dBSA (by dBSA : QD ratio at 6 : 1) and CdTe@TGA as a reference continually recorded over 16 days.

The optical stability was also investigated for exploring the application of CdTe@dBSA in immunofluorescence detection.[1,2,14,28] The fluorescence of the CdTe@dBSA particles in $1\times$ PBS was continually monitored. As shown in Fig. 3b, the fluorescence intensity remains almost unchanged over 16 days at room temperature. In huge contrast, the fluorescence of the parent CdTe QDs starts to steadily decline 4 days after, falls by 42% over 16 days. These results suggest that the dBSA coating can effectively enhance the optical stability of the CdTe QDs apart from enhancing the fluorescence QY. In addition, the fluorescence peak position remains unchanged as shown in ESI Fig. S2,† which suggests that dBSA coating also enhances the colloidal stability for the underlying CdTe core in physiological buffers.

3.2. Resistance of CdTe@dBSA to nonspecific adsorption

As aforementioned, dBSA coating is also expected to suppress the nonspecific adsorption of CdTe QDs on biointerfaces of its target. To show the antifouling effect of dBSA coating, CdTe@dBSA particles were incubated with fixed Raji cells for comparing with the CdTe@TGA QDs. As shown in Fig. 4, nearly no fluorescence is presented from the Raji cells incubated with CdTe@dBSA, contrasting to those incubated with CdTe@TGA QDs, which strongly implies the heavy nonspecific adsorption of the parent CdTe QDs can be effectively suppressed by the dBSA coating through blocking the vacant sites of biointerfaces.[46]
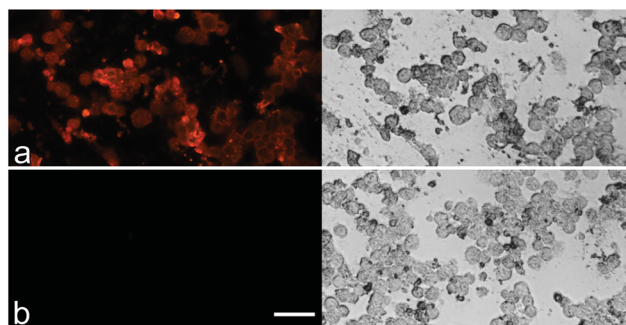

Fig. 4 Dark (left column) and bright field images (right column) of Raji cells incubated with CdTe@TGA row (a), and CdTe@dBSA row (b), respectively. The scale bar corresponds to 10 μm.

3.3. Conjugation of streptavidin to CdTe@dBSA

Apart from offering improved optical properties as well as good resistance to nonspecific adsorption, dBSA coating also provides sufficient functional groups for further conjugating the biospecific ligands to the QDs for the following immunofluorescence assays. To prevent the interparticle reactions during conjugation, the primary amine groups on CdTe@dBSA were converted to carboxyl groups by succinic anhydride.[32] The results were studied by 0.5% agarose gel electrophoresis. As shown in Fig. 5a, the succinylated CdTe@dBSA migrates noticeably faster than non-succinylated CdTe@dBSA, but remains slower than the CdTe@TGA QDs, implying the successful succinylation of free amino groups. Due to the enhanced density of negative charge on the surface of succinylated CdTe@dBSA, the electrophoretic mobility of succinylated CdTe@dBSA is increased in comparison with the non-succinylated CdTe@dBSA. Fig. 5b shows the fluorescence spectra of the original CdTe QDs, succinylated and non-succinylated CdTe@dBSA. Although the fluorescence intensity of the succinylated CdTe@dBSA is decreased in comparison to the non-succinylated CdTe@dBSA, but remains higher than that of CdTe@TGA QDs.

Streptavidin was chosen to construct the QD-based molecular probe because it can specifically bind to biotin and
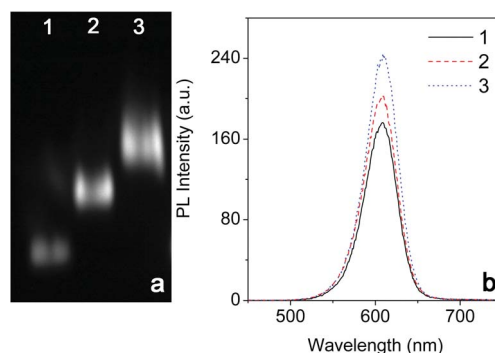

Fig. 5 (a) Gel electrophoresis images of CdTe QDs (Lane 1), succinylated CdTe@dBSA (Lane 2), and CdTe@dBSA before succinylation (Lane 3). (b) Fluorescence spectra of CdTe QDs (1), succinylated CdTe@dBSA (2) and CdTe@dBSA before succinylation (3).

biotinylated antibodies, and the streptavidin–biotin system has been widely used as an amplification technique in immunoassays.[47] Streptavidin was then conjugated with the carboxylate groups on CdTe@dBSA *via* an EDC/sulfo-NHS-mediated amidation reaction. The streptavidin-to-QD ratios of 1 : 2 and 1 : 1 were adopted. As a control, the mixture of streptavidin and QDs was also prepared to show the nonspecific interaction between streptavidin and CdTe QDs. The coupling reaction was evaluated by 1% agarose gel electrophoresis. As shown in Fig. 6, simply mixing streptavidin with QDs by molar ratios of 2 : 1 and 1 : 1 only give rise to slight variation in the electrophoretic mobility of the QDs. In contrast, conjugates of streptavidin and CdTe@dBSA obtained by molar ratio of 2 : 1 and 1 : 1 present decreased electrophoretic mobility, supporting the effective covalent coupling between streptavidin and CdTe@dBSA. Moreover, the resulting conjugate presents excellent stability under ambient conditions. It exhibits a time independent fluorescence intensity over 6 days as shown in Fig. S3.†

3.4. Detection of EBV infection in NPC by using CdTe@dBSA–streptavidin conjugate

Base on above optimizations, the resulting CdTe@dBSA–streptavidin conjugate was applied in detecting the serum level of VCA-IgA, which has been widely used for screening and diagnosing the EBV-associated cancers. As schematically shown in Fig. 7, the indirect immunofluorescence assay was adopted by using CdTe@dBSA–streptavidin conjugate as molecular probe. In principle, VCA-IgA existing in serum can be specifically captured by EBV expressed on activated Raji cells. The biotinylated antiIgA Ab will then specifically capture the CdTe@dBSA–streptavidin conjugate to enable the following detection.

The serum level of VCA-IgA of NPC patients with known EBV infection was detected with the sera from healthy donors serving as a negative control. The fluorescence microscopic results shown in Fig. 7 reveal that Raji cells incubated with the sera of NPC patients can be heavily stained by CdTe@dBSA. But not all of the Raji cells are stained because only 60–70% of Raji

Fig. 7 Upper panel: schematic drawing for illustrating the indirect immunofluorescence detection of VCA-IgA. Lower panel: dark (left) and bright (right) microscopic images of Raji cells treated by sera of NPC patients (a) and healthy donors (b), followed by biotinylated antiIgA Ab and CdTe@dBSA–streptavidin. The scale bar corresponds to 10 μm.

cells can be effectively activated to express EBV,[39] which further verifies the excellent binding specificity of the CdTe@dBSA–streptavidin conjugate. In huge contrast, the Raji cells incubated with sera from healthy donors present nearly no fluorescence upon the same staining process by using the CdTe@dBSA–streptavidin conjugate. These results suggest that the CdTe@dBSA-based indirect immunofluorescence assay can potentially be used for detecting the VCA-IgA from the EBV-infection serum, and thus provides an alternative approach for screening and diagnosing EBV-associated cancers.

4. Conclusion

In summary, dBSA has been successfully used to modify the CdTe QDs *via* ligand exchange process. Systematic studies reveal that the fluorescence intensity and optical stability of CdTe core can be significantly improved through the dBSA coating. Most importantly, the nonspecific adsorption of CdTe QDs on the membrane of carcinoma cells is effectively eliminated, which makes the CdTe@dBSA potentially useful for constructing high performance molecular probes for bioapplications. Through covalent bonding, streptavidin is attached to the surface of CdTe@dBSA to achieve a specific fluorescent probe that is capable of detecting the biomarker of EBV infection *via* indirect immunofluorescence assay. The excellent performance of the resulting probes not only offers an approach for detecting EBV-associated cancers, but also paves a
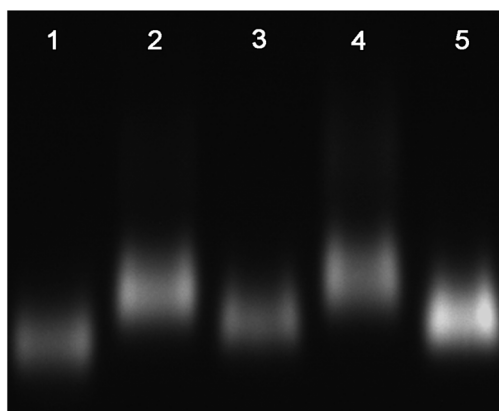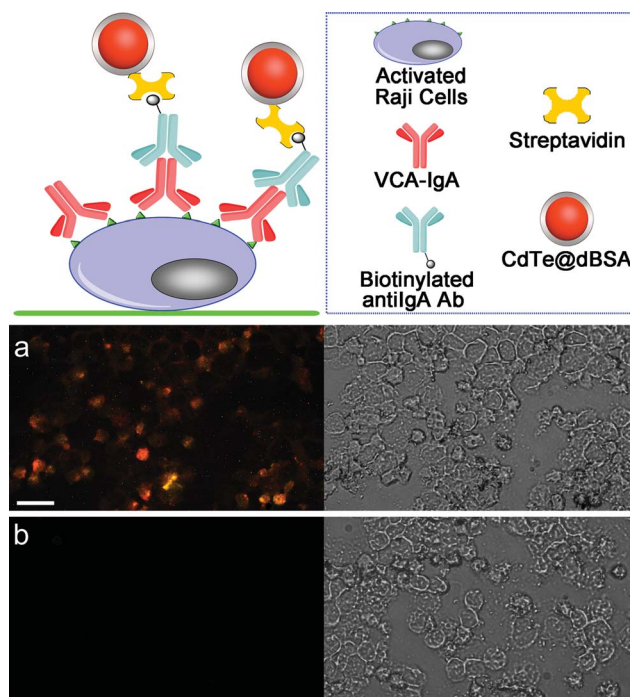

Fig. 6 Gel electrophoresis images of CdTe@dBSA (Lane 1), the conjugate (Lanes 2 and 4), and mixture (Lanes 3 and 5) of CdTe@dBSA and streptavidin by molar ratios of 2 : 1 (Lanes 2 and 3) and 1 : 1 (Lanes 4 and 5).

reliable way to construct different fluorescent probes for versatile *in vitro* assays.

Acknowledgements

References

1 P. Alivisatos, *Nat. Biotechnol.*, 2004, **22**, 47–52.

2 I. L. Medintz, H. T. Uyeda, E. R. Goldman and H. Mattoussi, *Nat. Mater.*, 2005, **4**, 435–446.

3 X. Michalet, F. Pinaud, L. Bentolila, J. Tsay, S. Doose, J. J. Li, G. Sundaresan, A. M. Wu, S. S. Gambhir and S. Weiss, *Science*, 2005, **307**, 538–544.

4 V. Biju, T. Itoh and M. Ishikawa, *Chem. Soc. Rev.*, 2010, **39**, 3031–3056.

5 B. Dubertret, P. Skourides, D. J. Norris, V. Noireaux, A. H. Brivanlou and A. Libchaber, *Science*, 2002, **298**, 1759–1762.

6 S. Kim, Y. T. Lim, E. G. Soltesz, A. M. De Grand, J. Lee, A. Nakayama, J. A. Parker, T. Mihaljevic, R. G. Laurence, D. M. Dor, L. H. Cohn, M. G. Bawendi and J. V. Frangioni, *Nat. Biotechnol.*, 2004, **22**, 93–97.

7 Y. Li, X. Duan, L. Jing, C. Yang, R. Qiao and M. Gao, *Biomaterials*, 2011, **32**, 1923–1931.

8 A. Y. Nazzal, X. Wang, L. Qu, W. Yu, Y. Wang, X. Peng and M. Xiao, *J. Phys. Chem. B*, 2004, **108**, 5507–5515.

9 J. A. Kloepfer, S. E. Bradforth and J. L. Nadeau, *J. Phys. Chem. B*, 2005, **109**, 9996–10003.

10 K. Boldt, O. T. Bruns, N. Gaponik and A. Eychmüller, *J. Phys. Chem. B*, 2006, **110**, 1959–1963.

11 M. J. Bruchez, M. Moronne, P. Gin, S. Weiss and A. P. Alivisatos, *Science*, 1998, **281**, 2013–2016.

12 M. E. Åkerman, W. C. Chan, P. Laakkonen, S. N. Bhatia and E. Ruoslahti, *Proc. Natl. Acad. Sci. U. S. A.*, 2002, **99**, 12617–12621.

13 B. Ballou, B. C. Lagerholm, L. A. Ernst, M. P. Bruchez and A. S. Waggoner, *Bioconjugate Chem.*, 2003, **15**, 79–86.

14 Y. Li, L. Jing, R. Qiao and M. Gao, *Chem. Commun.*, 2011, **47**, 9293–9311.

15 L. Liu, X. Guo, Y. Li and X. Zhong, *Inorg. Chem.*, 2010, **49**, 3768–3775.

16 P. Zrazhevskiy, M. Sena and X. Gao, *Chem. Soc. Rev.*, 2010, **39**, 4326–4354.

17 E. Pöselt, S. Fischer, S. Foerster and H. Weller, *Langmuir*, 2009, **25**, 13906–13913.

18 N. Zhan, G. Palui, M. Safi, X. Ji and H. Mattoussi, *J. Am. Chem. Soc.*, 2013, **135**, 13786–13795.

19 R. Gill, M. Zayats and I. Willner, *Angew. Chem., Int. Ed.*, 2008, **47**, 7602–7625.

20 H. T. Uyeda, I. L. Medintz, J. K. Jaiswal, S. M. Simon and H. Mattoussi, *J. Am. Chem. Soc.*, 2005, **127**, 3870–3878.

21 Y. Yang and M. Y. Gao, *Adv. Mater.*, 2005, **17**, 2354–2357.

22 Y. H. Yang, L. H. Jing, X. L. Yu, D. D. Yan and M. Y. Gao, *Chem. Mater.*, 2007, **19**, 4123–4128.

23 L. H. Jing, C. H. Yang, R. R. Qiao, M. Niu, M. H. Du, D. Y. Wang and M. Gao, *Chem. Mater.*, 2010, **22**, 420–427.

24 M. Kuang, D. Y. Wang, H. B. Bao, M. Y. Gao, H. Mohwald and M. Jiang, *Adv. Mater.*, 2005, **17**, 267–270.

25 Y. Gong, M. Gao, D. Wang and H. Möhwald, *Chem. Mater.*, 2005, **17**, 2648–2653.

26 Y. Yang, Z. Wen, Y. Dong and M. Gao, *Small*, 2006, **2**, 898–901.

27 Y. H. Yang, C. F. Tu and M. Y. Gao, *J. Mater. Chem.*, 2007, **17**, 2930–2935.

28 L. H. Jing, Y. L. Li, K. Ding, R. R. Qiao, A. L. Rogach and M. Y. Gao, *Nanotechnology*, 2011, **22**, 505104.

29 M. E. Åkerman, W. C. W. Chan, P. Laakkonen, S. N. Bhatia and E. Ruoslahti, *Proc. Natl. Acad. Sci. U. S. A.*, 2002, **99**, 12617–12621.

30 F. Hu, Y. Ran, Z. Zhou and M. Gao, *Nanotechnology*, 2006, **17**, 2972.

31 H. Kloust, C. Schmidtke, J. P. Merkl, A. Feld, T. Schotten, U. E. A. Fittschen, M. Gehring, J. Ostermann, E. Pöselt and H. Weller, *J. Phys. Chem. C*, 2013, **117**, 23244–23250.

32 Q. Wang, Y. Kuo, Y. Wang, G. Shin, C. Ruengruglikit and Q. Huang, *J. Phys. Chem. B*, 2006, **110**, 16860–16866.

33 Y. C. Kuo, Q. Wang, C. Ruengruglikit, H. Yu and Q. Huang, *J. Phys. Chem. C*, 2008, **112**, 4818–4824.

34 A. G. Papavassiliou and D. Bohmann, *Nucleic Acids Res.*, 1992, **20**, 4365–4366.

35 Y. Wang, K. El-Boubbou, H. Kouyoumdjian, B. Sun, X. Huang and X. Zeng, *Langmuir*, 2010, **26**, 4119–4125.

36 S. H. Brorson, *Micron*, 1997, **28**, 189–195.

37 M. P. Thompson and R. Kurzrock, *Clin. Cancer Res.*, 2004, **10**, 803–821.

38 G. Henle and W. Henle, *Int. J. Cancer*, 1976, **17**, 1–7.

39 Y. Zeng, J. Zhong, L. Li, P. Wang, H. Tang, Y. Ma, J. Zhu, W. Pan, Y. Liu and Z. Wei, *Intervirology*, 1983, **20**, 190–194.

40 M. Gao, S. Kirstein, H. Möhwald, A. L. Rogach, A. Kornowski, A. Eychmüller and H. Weller, *J. Phys. Chem. B*, 1998, **102**, 8360–8363.

41 A. L. Rogach, T. Franzl, T. A. Klar, J. Feldmann, N. Gaponik, V. Lesnyak, A. Shavel, A. Eychmüller, Y. P. Rakovich and J. F. Donegan, *J. Phys. Chem. C*, 2007, **111**, 14628–14637.

42 A. Shavel, N. Gaponik and A. Eychmüller, *J. Phys. Chem. B*, 2006, **110**, 19280–19284.

43 X. Gao, W. C. Chan and S. Nie, *J. Biomed. Opt.*, 2002, **7**, 532–537.

44 H. Bao, Y. Gong, Z. Li and M. Gao, *Chem. Mater.*, 2004, **16**, 3853–3859.

45 W. W. Yu, L. Qu, W. Guo and X. Peng, *Chem. Mater.*, 2003, **15**, 2854–2860.

46 A. Iordanskii, V. Markin, L. Razumovskii, R. Y. Kosenko, N. Tarasova and G. Zaikov, *Desalination*, 1996, **104**, 113–118.

47 P. C. Weber, D. H. Ohlendorf, J. J. Wendoloski and F. R. Salemme, *Science*, 1989, **243**, 85–88.